IET Microwaves, Antennas & Propagation

*Research Article*

IET Journals
The Institution of Engineering and Technology

# Pattern diversity antenna with high-temperature tolerance for body area networks

ISSN 1751-8725
Received on 21st May 2015
Revised on 18th August 2015
Accepted on 1st September 2015
doi: 10.1049/iet-map.2015.0342
www.ietdl.org

*Alam Muhammad Faiz[1], Nayab Gogosh[2], Abdul Rehman[3], Muhammad Farhan Shafique[3] ✉, Benoit Poussot[1], Jean Marc Laheurte[1]*

[1]*Laboratoire ESYCOM, University of Paris Est, Champs-sur-Marne, France*
[2]*Department of Electrical Engineering, COMSATS Institute of Information Technology, Park Road, Tarlai Kalan, Islamabad 45550, Pakistan*
[3]*Center for Advance Studies in Telecommunications, COMSATS Institute of Information Technology, Park Road, Tarlai Kalan, Islamabad 45550, Pakistan*
✉ *E-mail: farhan.shafique@comsats.edu.pk*

**Abstract:** A high-temperature tolerant pattern diversity antenna is presented for body wearable applications in hostile conditions. The proposed system consists of a dielectric resonator antenna (DRA) placed at the centre of a slot loop antenna. The combination yields pattern diversity with broadside and endfire radiation patterns from slot loop and DRAs, respectively. The antenna system offers common bandwidth of 4.95% with port isolation of better than 13 dB at 2.4 GHz. The thermal characteristics of antenna have been studied for high-temperature operation and no discernible change in the radiation behaviour is noted. The antenna undergoes 2% resonant frequency shift when operated at elevated temperature. The antenna diversity has been measured for three on-body communication channels. The antenna offers 9.5 dB diversity gain in a pure non-line-of-sight channel surrounded by a rich fading environment subjected to the selection combining scheme. The antenna has dimensions of $0.4\lambda_o \times 0.4\lambda_o \times 0.1\lambda_o$.

## 1 Introduction

The reliability of wireless links is of prime importance when it comes to their applications in critical conditions. Diversity antennas are gaining popularity owing to their ability of providing a reliable communication link. There are certain applications where wearable diversity antennas are best suited, for example, in a real-time patient monitoring system [1]. In a similar fashion, rescue workers or fire fighters under hostile conditions require a reliable communication link with their base station. These extreme applications require specially designed antennas which could withstand harsh environmental conditions such as high temperature or humidity. Therefore, there remains a need of such antennas which not only offer diversity performance but also withstand high temperature and harsh conditions.

There are various high-temperature tolerant antennas that have been proposed for harsh temperature conditions like in [2] platinum have been used on alumina substrate to make it operational at extreme temperature; due to platinum the antenna had high ohmic loss. In another study, a detailed characterisation of folded dipole antenna made of gold on alumina substrate was carried out for temperature range of 25–400°C. It has been reported that 1% resonant frequency shift was observed [3].

A number of single- and dual-element antennas have been proposed for body area network (BAN) applications. They cover different aspects and different applications of body centric communications. In [4], a detailed analysis of different diversity schemes has been conducted for on-body communications channels at 2.45 GHz. Planar inverted F antennas and printed inverted F antennas have been used to compute the diversity gain (DG) and correlation coefficient.

Non-planar antennas have also been investigated for BAN application for narrow and ultra-wideband applications [5, 6]. Most of the research focused on BAN so far discusses better common impedance bandwidths or DG techniques [4–8]. These antennas are intended for normal operating conditions and they have no established thermal analysis.

Dielectrics are known for their ruggedness and high-temperature tolerance as compared with metals, therefore a DRA can perform at much elevated temperature as compared with a metallic counterpart. In this work, a dual radiation pattern antenna, comprising of broadside radiation originating from a co-planar waveguide (CPW) fed slot-loop [9] and endfire radiation produced by a probe fed DRA [10] is investigated for high-temperature applications. The slot loop antenna loaded with DRA was first proposed in [11]. This work analyses the performance of the proposed diversity antenna for different on-body channels and its potential application in harsh temperature conditions.

## 2 Antenna geometry

The proposed antenna consists of a slot loop radiator covered with a DRA as shown in Fig. 1. The slot loop antenna radiates in the broadside direction and it is fed with a CPW. The DRA placed at the centre of the slot loop antenna is fed with a monopole inserted in the centre from bottom. This excitation mechanism of DRA produces TM01δ mode resulting in an endfire (or monopole alike) radiation pattern [12]. The DRA remains confined within the area of slot loop. The loading of DRA at centre serves various important objectives; it lowers the resonant frequency of slot loop antenna and helps it to achieve the same resonant frequency with 19.3 mm radius instead of 23.5 mm. Also the DRA loading enhances the impedance bandwidth of slot loop antenna from 2.5 to 4%. A very important effect of DRA loading is the masking of exposed metal to high temperature, thus improving the temperature tolerance of the slot loop antenna.

A circular disc of 3 mm diameter in the centre of slot loop was etched to isolate the feeding probe of DRA from shortening with the surrounding ground plane. The effects of adhesive materials used to bond DRA have been taken into account by adding a layer of 200 μm epoxy in simulations [13]. The design was simulated and optimised using Ansys High Frequency Structured Simulator.

## 3 Thermal analysis

Since the objective is to deploy the proposed antenna in high-temperature environment, the thermal analysis of the material

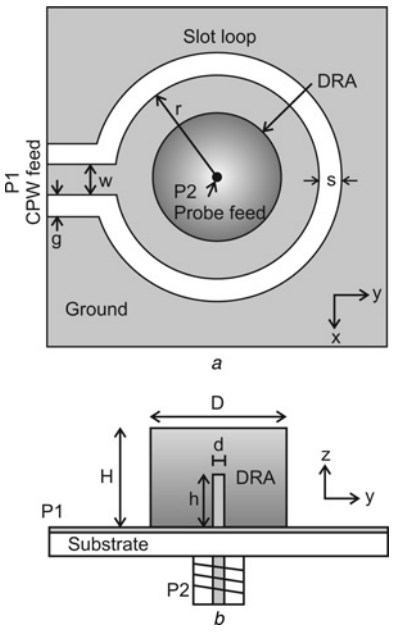


**Fig. 1** *Antenna geometry*

*a* Top view
*b* Side view
Dimensions are $r = 19.3$ mm, $s = 0.7$ mm, $w = 4.2$ mm, $g = 1.5$ mm, $D = 30$ mm, $H = 12$ mm, $d = 1$ mm and $h = 7$ mm

was carried out at ambient temperature of 400°C. Generally in high-temperature microwave applications, the relevant parameters to be investigated are thermal conductivity, thermal expansion, variation in conductivity and variation in dielectric constant. A material tends to expand when exposed to high temperature and this expansion is governed by the relations given in the following equations [14]

$$\Delta A = 2\alpha A \Delta T \tag{1}$$

$$\Delta V = 3\alpha V \Delta T \tag{2}$$

where $\alpha$ is the coefficient of linear expansion, for copper it is 17 ppm/°K, for DRA material it is 36 ppm/°K and for substrate material (RO4003) it is 11, 14 and 46 ppm/°K for $x$, $y$ and $z$ dimensions, respectively. Based on the expansion relations only 4% change has been predicted in the volume of DRA at 400°C.

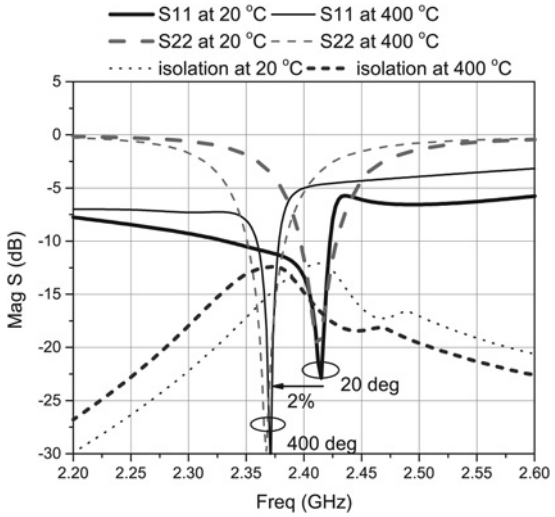


**Fig. 2** *Simulated S-parameters at 20 and 400°C*

Similarly, slot loop antenna tends to vary by 1.3% and the substrate thickness varies by 1.7% only. The DRA material is also expected to limit the expansion of the under laid copper clad upon which slot loop is etched.

Conductivity reduces with rise in temperature, and this variation is predicted by the relation given in the following equation[14]

$$\sigma_{CU} = \frac{\sigma_{ref}}{1 + \alpha(T - T_{ref})} \tag{3}$$

where $T_{ref}$ is reference temperature usually 20°C and $\sigma_{ref}$ is conductivity at reference temperature and $\alpha$ is the temperature coefficient of resistance. The reference conductivity of copper is $5.96 \times 10^7$ S/m and $\alpha$ is 0.0038/°C, and the expected conductivity at 400°C will reduce to $2.44 \times 10^7$ S/m.

Likewise the thermal coefficient of $\epsilon_r$ for Rogers 4003 substrate used in this study is 40 ppm/°C with specified rated variation of 0.5% in $\epsilon_r$ at 400°C and for DRA the variation is <3% [15].

Considering all the possible variations for the worst case scenario in physical dimensions and electrical properties at 400°C, a simulation was carried out to observe the scattering parameter behaviour at elevated temperature. The result of the simulation is shown in Fig. 2.

The behaviour in Fig. 2 is predictable since the permittivity increases with temperature and the resonant frequency tends to shift towards lower frequency and also the quality factor tends to improve [16]. The proposed antenna structure limits this change to only 2% (50 MHz) due to its physical geometry and temperature distribution.

The thermal analysis was conducted using commercially available multiphysics tool COMSOL™. Copper has thermal conductivity of 385 W/mK, while the ceramic DRA used in this study has thermal conductivity of only 0.4 W/mK.

The graph presented in Fig. 3 reflects the behaviour of temperature variation on the antenna. The maximum temperature observed on the surface of DRA and copper is plotted with respect to the time of exposure. The maximum and minimum temperature simulated on the shielded copper underneath the DRA is also plotted.

It can be seen that the copper surface exposed to the environment has undergone a rapid increase in temperature as compared with the DRA. The copper temperature is 100°C more than that of the DRA for the first 30 min, and later reduces to about 50°C higher in the next 30 min. The copper portion that is covered with the DRA has equal or lower temperature as compared with the DRA. However, at the edge of the shielded copper, the temperature is slightly higher than the DRA. This leads to the conclusion that DRA not only undergoes slower temperature rise but it also protects the portion of ground plane that it covers. The temperature distribution over different antenna surfaces is presented in Fig. 4. A noticeable

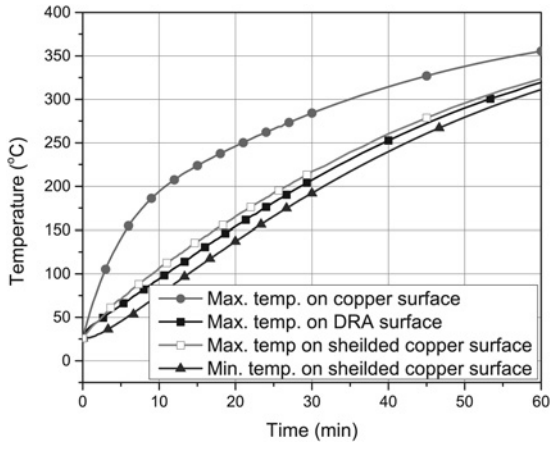


**Fig. 3** *Simulated temperature variations on various antenna surfaces, from COMSOL™*

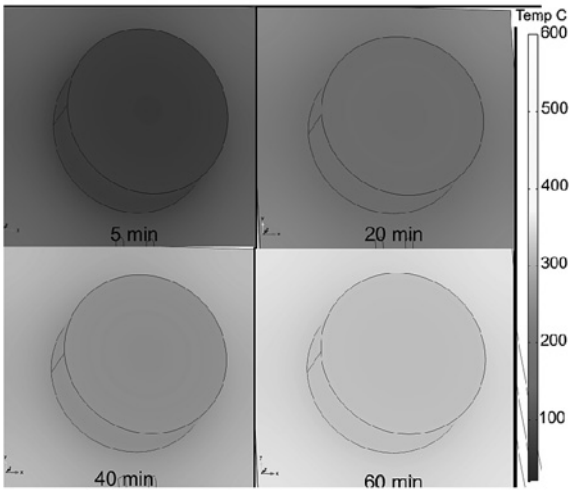


**Fig. 4** *Temperature distribution on different antenna surfaces*

temperature variation can be seen between DRA and copper surface that is exposed to the ambient air.

## 4 Fabrication and measurements

The antenna was fabricated on RO4003 substrate with $\epsilon_r$ of 3.38 and tan $\delta$ of 0.0027. The substrate thickness was 0.508 mm. The DRA was made from commercially available material (ECCOSTOCK HIK 500F by Emerson and Cuming) with $\epsilon_r$ of 30 and tan $\delta$ of 0.002. Considering the application of antenna in BANs, it has been analysed by simulating on a human phantom with a separation of 10 mm from the body. The human phantom model was generated with a uniform layer of muscle with $\epsilon_r$ of 54.5 and $\sigma = 1.84$ S/m [17, 18]. The antenna measurements were performed at normal temperature instead of 400°C, as simulation results concluded that there is a little variation in the resonant frequency which can be incorporated in the design prior to fabrication. The return losses and isolation curves are presented in Fig. 5. The measured 10 dB return loss ranges from 2.34 to 2.73 GHz for slot loop and from 2.36 to 2.48 GHz for DRA. It thus yields the common impedance bandwidths of 4.95% centred on the working frequency of 2.4 GHz with port isolation of 13 dB. The enhancement in the bandwidths of measured results is attributed to the DRA loading tolerance and adhesive material losses that reduces the $Q$ factor.

The radiation pattern of slot loop antenna is presented in Fig. 6. The simulated on-body antenna shows broadside radiation pattern with maximum radiation at $\theta = 0°$. There is low radiation on the backside due to the presence of human phantom. Fig. 6*b* shows the measured free-space radiation pattern of slot loop antenna, and the broadside radiation pattern can be observed with cross-polar components of −10 dB or smaller magnitudes.

The simulated DRA radiation pattern on human phantom is presented in Fig. 7. A clear endfire radiation pattern can be observed for the DRA. The cross-polar component is <13 dB. A slightly distorted endfire radiation pattern when measured in free space was observed as shown in Fig. 7*b*. The asymmetry is related to the effects of slot loop feeding connector. However, it is worth noting that there is a null in the broadside direction which will reduce the coupling with the radiation pattern of slot loop radiator.

A comparison of DRA and slot loop antenna radiation patterns is presented in Fig. 8 for room-temperature and high-temperature operation. It has been observed that elevated temperature causes little effect on antenna gain and radiation pattern. Since the variation in temperature does not affect the excited mode in DRA, therefore the resultant radiation pattern remains unchanged. The peak gain for DRA at room temperature in endfire direction ($\theta = 90°$) is 1.25 dBi and at 400°C the peak gain is found to be 0.19

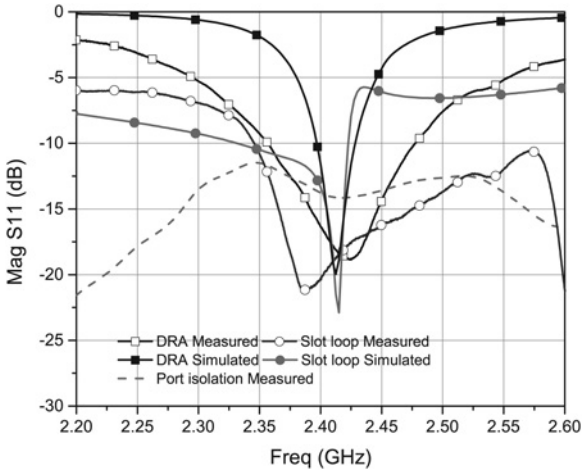


**Fig. 5** *On-body measured return loss and isolation curves*

dBi. However, for slot loop antenna there is a slight variation in radiation pattern in the broadside direction ($\theta = 0°$) where the gain is reduced by 4 dB from −0.1 dBi at room temperature to −4.1 dBi at 400°C. This variation is caused by the slight expansion of copper which reduces the gap of radiating slot. It can be observed that slot loop antenna at high temperature has increased gain around 110° which is expected to slightly reduce the DG in non-line of sight (NLOS) channel.

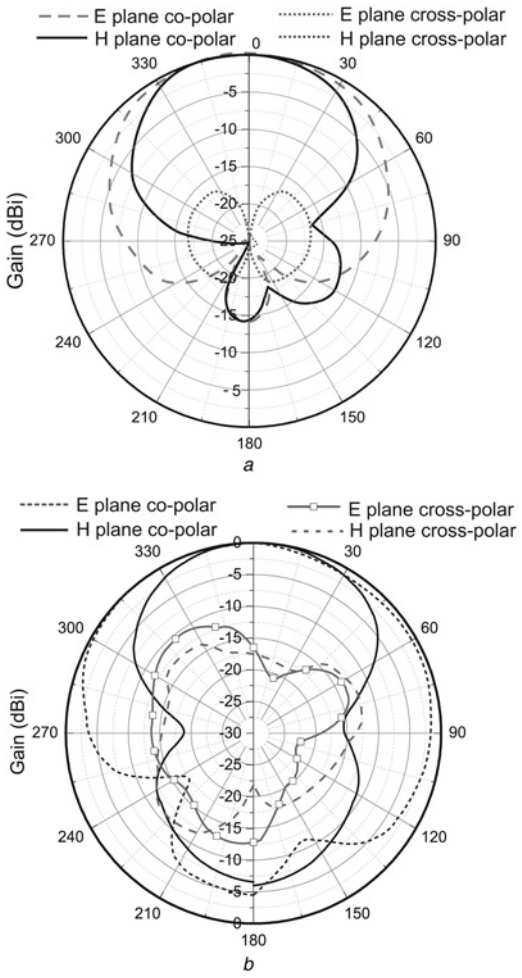


**Fig. 6** *Slot loop radiation patterns*

*a* Simulated on body
*b* Measured in free space

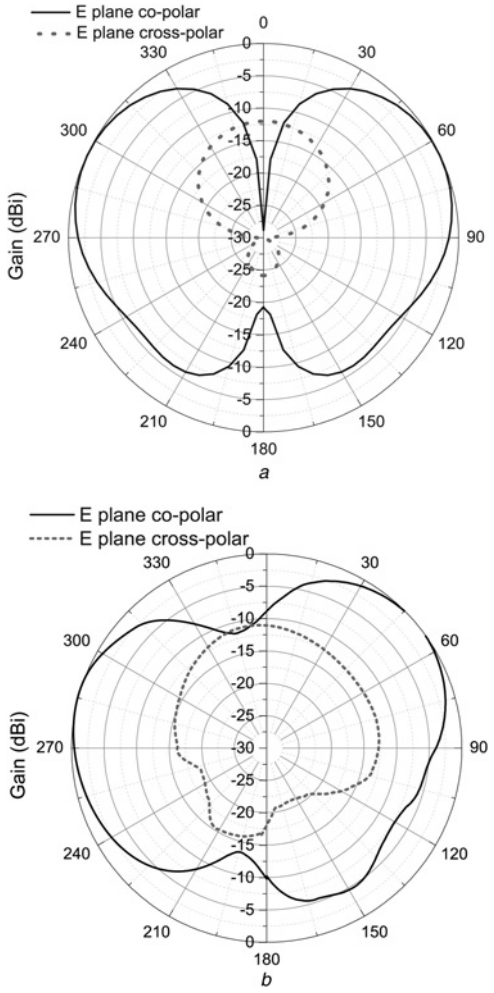


**Fig. 7** *DRA radiation patterns*

*a* Simulated on body
*b* Measured in free space

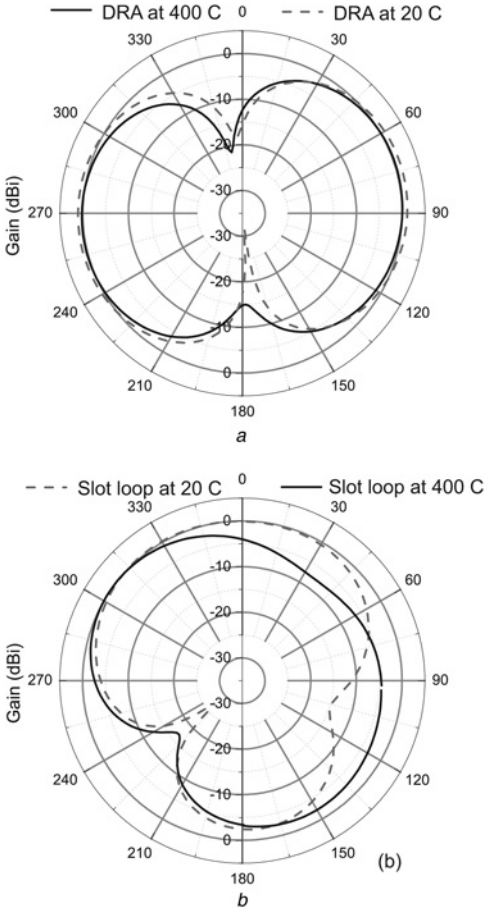


**Fig. 8** *Effect of temperature variation on radiation patterns*

*a* DRA
*b* Slot loop antenna

## 5 DG measurement

The performance of the proposed on-body diversity antenna has been evaluated by deploying it in receiving mode at three different positions which are chest, abdomen side and back. For all these placements, the transmitting antenna was installed on waist at belly position. These are the common positions that soldiers or firemen wearing special protective kits can spare for this purpose. There are three possible communication links: line of sight (LOS), partial LOS and indirect or NLOS. In order to realise these three channels inside a rich scattering environment of laboratory, both the transmitting and receiving antennas are added to the human body. The transmitting and receiving antennas are added to different positions on body to mimic the three channels. For pure LOS channel both transmitter and receiver has to be in visual contact with one another, therefore the receiving antenna which is in this case the DRA is placed on the chest of human body and transmitting antenna is fixed on belly position. This combination of both antennas produces a LOS channel. Similarly for partial LOS channel the receiving DRA is placed on the side of human body. This combination allows certain signal to reach the receiving antenna directly from transmitter and a portion of signal reaches there after scattering from the environment. This makes the effect of partial LOS channel. Likewise for pure NLOS channel the receiving DRA is placed on the back side of human body, thus removing any LOS communication with the transmitter. The only possibility of reaching the signal from transmitter to receiver is through reflection and scattering from the environment, thus realising a pure NLOS channel. In all these measurements, a

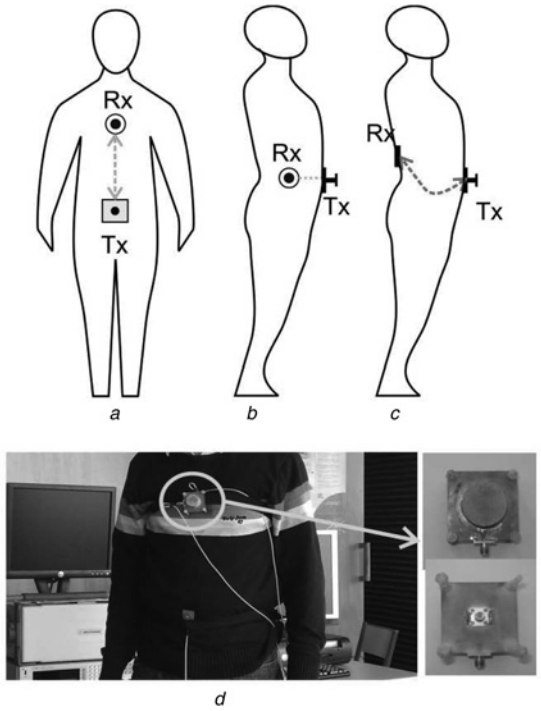


**Fig. 9** *Location of three on-body channels*

*a* LOS
*b* Partial LOS
*c* NLOS
*d* Subject with diversity antenna worn at chest and transmitter worn at belly position

standard monopole antenna operating at at 2.4 GHz with 0 dBm power was used. The locations of these channels are elaborated in Fig. 9.

The abundance of various objects randomly located inside the laboratory setup provides a fully rich fading environment to perform diversity analysis. The replica of signals reflected from these objects comprises of various amplitudes and phases that are received at the diversity antenna. This scattering environment makes broadside radiating antenna to be more receptive for the signals normal to the antenna and endfire radiating antenna for the signal parallel to the antenna. The received signals were combined using selection combining (SC) technique. The combined data was then used to plot cumulative distribution function (CDF). With reference to these CDFs, a shift from a stronger branch signal to the combined signal at an outage probability of 1% is referred to as DG. These three on-body channels were individually studied for their DG and correlation coefficient performances. Since the antenna is meant to be embedded in a protection suite, it is planted at a height of 10 mm under which a clothing pad was used.

The vector network analyser was calibrated in the power reception mode for a sample time period of 60 s. The person under test was planted with transmitting and receiving antennas in order to imitate the three possible on-body channels. The subject was made to perform random motions with normal walking speed so as to receive effectively the signals faded by the surrounding laboratory's multi-path environment.

### 5.1 Belly–chest channel

In this on-body channel, the diversity antenna was mounted on the chest of human body and it was in LOS with the transmitting monopole at belly position. The DG is observed to be zero for this scheme because of LOS link between transmitting and receiving antennas and after combining, it offers a clear power imbalance (in favour of DRA) which then failed to provide any diversity advantage. The individually received power and their combination are presented in Figs. 10*a* and *b*. It can be noted that the signal power received by DRA is more than the power received by the slot loop antenna so by using SC technique no DG is achieved. This is verified by plotting the CDF of the received signals (Fig. 10*c*). There is no DG and the combined power and DRA received power were the same. The envelope correlation coefficient (Fig. 10*d*) for this body channel remains below 0.3 due to LOS factor.

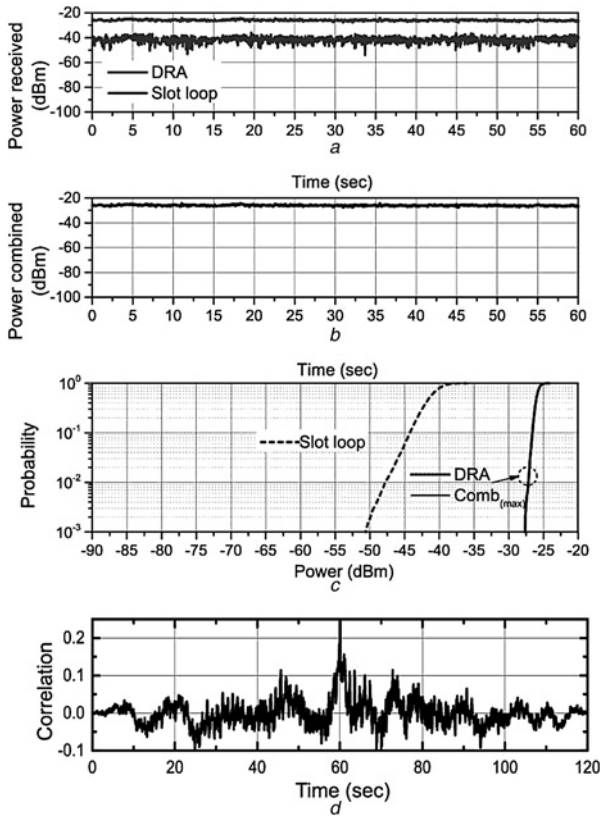


**Fig. 10** *Measured belly–chest channel*

*a* Received powers
*b* Combined power
*c* CDF for DG
*d* Envelope correlation coefficient

### 5.2 Belly–abdomen side channel

For belly to abdomen side channel, a DG of 2 dB was observed since the link was partially LOS and partially NLOS, so due to the contribution of faded signals approaching the antenna, a lesser power imbalance favoured a little improvement in DG value. The received signal power by DRA and slot loop antenna along with their combination are presented in Figs. 11*a* and *b*. The CDF for this scheme is presented in Fig. 11*c* which shows a slight improvement from comparatively stronger DRA signal to CDF curve of combined signal. The envelope correlation coefficient for this channel is reduced to 0.1 (Fig. 11*d*) as a result of partial LOS between source and receiver.

### 5.3 Belly–back channel

For belly to back link, a DG of ~9.5 dB was observed since both antennas were in the NLOS condition and both branches of the diversity antenna independently collected signals scattered from the surrounding objects. This mechanism totally eliminates the

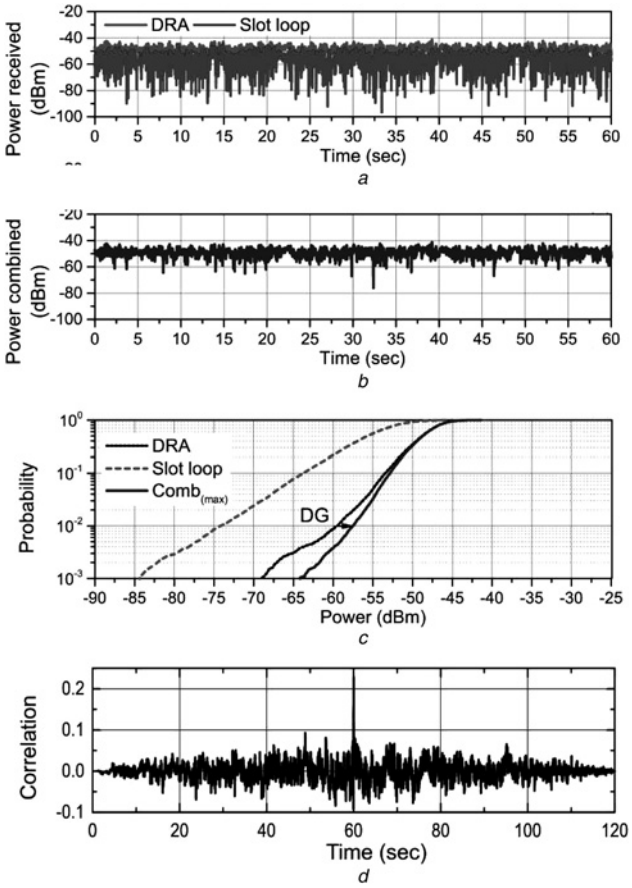


**Fig. 11** *Measured belly–abdomen side channel*

*a* Received powers
*b* Combined power
*c* CDF for DG
*d* Envelope correlation coefficient


*IET Microw. Antennas Propag.*, 2016, Vol. 10, Iss. 2, pp. 162–167

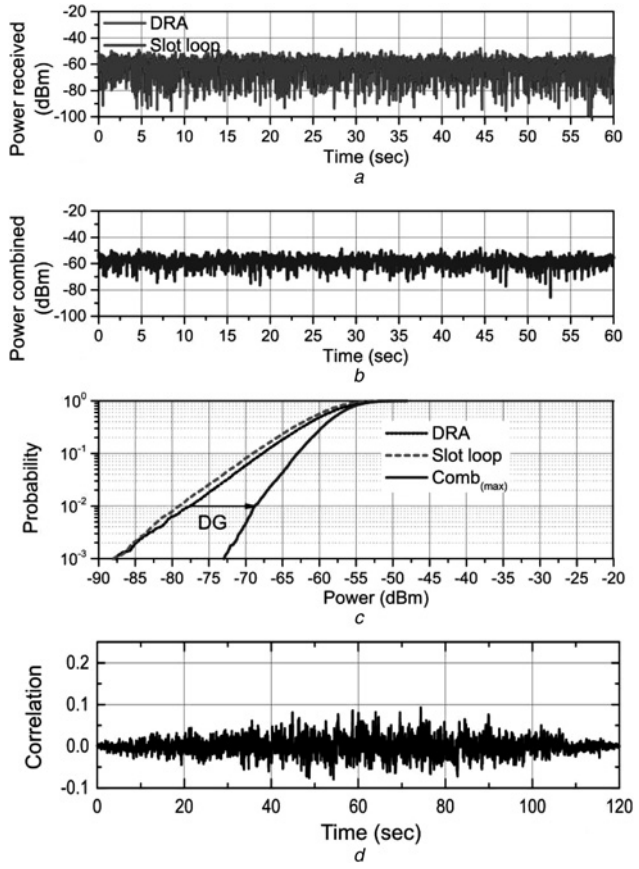


**Fig. 12** *Measured belly–back channel*

*a* Received powers
*b* Combined power
*c* CDF for DG
*d* Envelope correlation coefficient

power imbalance factor in which SC technique gives nearly equal weight to both branches, thus introducing a larger DG value. This is presented in Fig. 12. Due to NLOS condition, the envelope correlation coefficient for this channel remains below 0.1 as shown in Fig. 12*d*.

The DRA undergoes no considerable change in performance at 400°C as compared with room temperature apart from 2% resonant shift. This resonant shift can be rectified straight away by scaling the design by considering the intended frequency of operation. This study backed by the detailed analysis of thermal properties of material through multi-physics simulations endorses the performance of DRA at high temperature. On the other hand, the measurement of the prototype at such high-temperature conditions is hard to conduct. So as far as its real-time use is concerned, it is expected not to undergo any drastic change.

## 6 Conclusion

The pattern diversity antenna consisting of a DRA and a slot loop radiator has been analysed for high-temperature conditions. The pattern diversity has been achieved by mounting a DRA on the top of slot loop antenna which results in an endfire and broadside radiation patterns, respectively. The detailed analysis on antenna thermal characteristics when exposed to high temperature has been carried out. A significant temperature variation has been observed for the period of first 30 min when the copper was at 100°C higher temperature as compared with DRA and even after 60 min the DRA still had 50°C less temperature then copper. The diversity analysis shows that the antenna is an excellent candidate for NLOS body wearable applications where a DG of 9.5 dB has been achieved. A small footprint of antenna makes it suitable to be embedded into various locations available in the specially designed equipment kits worn by soldiers and firemen. Utmost care is required to fabricate the antenna to ensure repeatability since the DRA is probe fed and TM01δ is a higher order mode, therefore other DR modes can be unintentionally excited resulting in degradation of antenna response. The proposed antenna is mounted on safety suites, therefore its radiation characteristics is affected by the material that is used for the suite. The back radiation of the slot loop is the main effected parameter, and it may result in diffraction and causing degradation in the main lobe of antenna and resulting in the reduction of DG. To cater for this problem, a compact packaging can be introduced around antenna which has a suitable low permittivity backing material underneath the antenna to suppress the effects of clothing.

## 7 References


1 Rahim, A., Karmakar, N.C.: 'Measurement of correlation coefficient for dynamic WBAN channels in sleep apnoea monitoring system'. Proc. of 6th Int. Conf. on Broadband Communications & Biomedical Applications, 2011, pp. 246–251
2 Cheng, H., Ren, X., Ebadi, S., *et al.*: 'A wide-band square slot antenna for high temperature applications'. Proc. of Int. Symp. of IEEE Antennas and Propagation Society, 2014, pp. 242–243
3 Scardelletti, M.C., Jordan, J.L., Ponchak, G.E.: 'Temperature dependency (25 C–400 C) of a planar folded slot antenna on alumina substrate', *IEEE Antennas Wirel. Propag. Lett.*, 2008, **7**, pp. 489–492
4 Khan, I., Hall, P.S., Serra, A.A., *et al.*: 'Diversity performance analysis for on-body communication channels at 2.45 GHz', *IEEE Trans. Antennas Propag.*, 2009, **57**, (4), pp. 956–963
5 Kang, C.H., Wu, S.J., Tarng, J.H.: 'A novel folded UWB antenna for wireless body area network', *IEEE Trans. Antennas Propag.*, 2012, **60**, (2), pp. 1139–1142
6 Klemm, M., Kovcs, I., Pedersen, G.F., *et al.*: 'Novel small-size directional antenna for UWB WBAN/WPAN applications', *IEEE Trans. Antennas Propag.*, 2005, **53**, (12), pp. 3884–3896
7 Kang, C.H., Wu, S.J., Tarng, J.H.: 'Novel folded UWB antenna for wireless body area network', *IEEE Trans. Antennas Propag.*, 2012, **60**, (2), pp. 1139–1142
8 Klemm, M., Troester, G.: 'Textile UWB antennas for wireless body area networks', *IEEE Trans. Antennas Propag.*, 2006, **54**, (11), pp. 3192–3197
9 Chen, J.S., Chen, H.D.: 'Dual-band characteristics of annular-ring slot antenna with circular back-patch', *IET Electron. Lett.*, 2003, **39**, (6), pp. 487–488
10 Guo, Y.X., Ruan, Y.F., Shi, X.Q.: 'Wideband stacked double annular ring dielectric resonator antenna at the end fire mode operation', *IEEE Trans. Antennas Propag.*, 2005, **53**, (10), pp. 3394–3397
11 Faiz, A.M., Alves, T., Poussot, B., *et al.*: 'A diversity antenna combining slot-loop DRA for BAN applications', *IET Electron. Lett.*, 2012, **48**, (1), pp. 7–8
12 Long, S., McAllister, M., Shen, S.: 'The resonant cylindrical dielectric cavity antenna', *IEEE Trans. Antennas Propag.*, 1983, **31**, (3), pp. 406–412
13 Faiz, A.M., Gogosh, N., Khan, S.A., *et al.*: 'Effects of an ordinary adhesive material on radiation characteristics of a dielectric resonator antenna', *Microw. Opt. Technol. Lett.*, 2014, **56**, (6), pp. 1502–1506
14 Halliday, D., Resnik, R., Krane, K.: 'Physics' (John Wiley & Sons Inc., 2003, 5th edn.)
15 'Technical bulletin, EK-025 Eccostock HIK-500F', Emerson and Cuming
16 Dong, Y., Itoh, T.: 'Planar ultra-wideband antennas in Ku- and K-band for pattern or polarization diversity applications', *IEEE Trans. Antennas Propag.*, 2012, **60**, (6), pp. 2886–2895
17 Klemm, M., Kovacs, I.Z., Pedersen, G.F., *et al.*: 'Comparison of directional and omni-directional UWB antennas for wireless body area network applications'. Proc. of 18th Int. Conf. on Applied Electromagnetics and Communications, 2005, pp. 1–4
18 Gabriel, C.: 'Compilation of the dielectric properties of body tissues at RF and microwave frequencies'. U.S. Air Force Report AFOSR-TR-96, 1996